

DIFFERENT IMAGING MODALITIES USED FOR THE DETECTION OF PROSTATE CANCER – A REVIEW

Mr. Yash Shah¹, Mrs. Raksha K. Patel², Dr. Anand Mankodia³, Dr. Vipul A. Shah⁴,
Dr. Manish Thakker⁵

¹Research Scholar, M. Tech Biomedical Engineering, U V Patel College of Engineering, Ganpat University, Kherva, Gujarat, India.

²Associate Professor, Department of Biomedical Engineering, U V Patel College of Engineering, Ganpat University, Kherva, Gujarat, India.

³Associate Professor, Department of Electronics & Communication Engineering, U V Patel College of Engineering, Ganpat University, Gujarat, India.

⁴Professor, Department of Instrumentation & Control Engineering, Dharmsinh Desai University, Nadiad, Gujarat, India.

⁵Professor, Department of Instrumentation & Control Engineering, L. D. College of Engineering, Ahmedabad, Gujarat, India.

Abstract - Most common site for cancer is prostate, for example, of the 184,500 newly diagnosed instances of cancer in men which constitutes 29% of new cases. The patient's age, general health, the type and stage of cancer present, the treatment's potential side effects, and the patient's and doctor's personal preferences are all important considerations when deciding on a course of action. In this article, we will take a look back at the main imaging techniques used to diagnose and localize prostate cancer, including multiparametric ultrasound (US), multiparametric magnetic resonance imaging (MRI), MRI-US fusion imaging, and positron emission tomography (PET) imaging. The biological and functional properties of tumors that justify the application of a given imaging modality are given primary consideration. T2-weighted MRI and anatomical grayscale US can reveal alterations in tissue architecture. Doppler and contrast-enhanced ultrasound (US) as well as dynamic contrast-enhanced magnetic resonance imaging (MRI) take advantage of the fact that tumor growth is aided by angiogenesis. Clinical staging with the DRE and PSA is not very precise; however, imaging modalities like TRUS and MRI can improve this.

Key Words: Prostate, Cancer, Treatment, Fusion, Imaging.

1. INTRODUCTION

In men, prostate cancer is the second most prevalent type of cancer that ultimately results in death. The rate of prostate cancer, which is measured in instances per 100,000 males, has remained reasonably stable at 165. Early diagnosis and treatment are credited for the 31% decline in the age-adjusted death rate that has occurred since 1990 [1]. This decline can be attributable to the fact that more people are living longer. The diagnosis of prostate cancer has been changed to a lower grade, organ-confined disease as a result of prostate screening with digital rectal examination (DRE) and prostate-specific antigen (PSA) [2, 3]. This has contributed to the over detection and overtreatment of prostate cancer by at least 30 percent [4]. Recent research conducted by Etzioni and colleagues estimated that 10% of men with low-grade prostate cancer underwent unnecessary radical surgery, while 45% of these same men underwent unnecessary radiation therapy. As a result of the publication of the 10-year results of the Prostate, Lung, Colorectal, and Ovarian (PLCO) Cancer Screening Trial demonstrating that there was no reduction in mortality with screening, the new challenge is in differentiating clinically relevant tumors from ones that may otherwise never have become evident if it were not for screening. Because of the rapid advancement of imaging technologies, prostate cancer may now be detected and staged more accurately, which paves the way for more targeted treatment and subsequent monitoring. However, the correct use of imaging is difficult to pin down due to the numerous contentious studies that can be found in the published literature concerning each of the modalities and the utilities that they offer. In this section, we will cover the imaging techniques that are considered to be more established, and we will review various imaging techniques that show promise for the future.

1.1 PROSTATE ANATOMY AND CANCER

In order to set the stage for our discussion of the various imaging modalities for the prostate, we will first briefly digress to cover the morphology of the prostate, pathology grading, and therapy choices for PCa.

The structure of the prostate. The rectum covers the prostate gland from behind, while the bladder covers it from above. The urethra is partially encircled by the gland. Base refers to the end of the gland closest to the bladder, whereas apex describes the end of the gland closest to the external urethral sphincter. The prostate is divided into four anatomical regions called McNeal zones: the peripheral zone (PZ), which contains about 70% of glandular tissue; the transition zone (TZ), which contains about 5% of glandular tissue; the central zone (CZ), which contains about 25% of glandular tissue; and the anterior fibromuscular stroma, which contains about 0% glandular tissue (Fig. 1A). PCa incidence rates are as follows: 68% in the PZ, 24% in the TZ, and 8% in the AZ (CZ). 4 Image-guided interventional procedures, such as a prostate biopsy, make it simple to identify these areas.

Grading of PCa pathology. As was previously noted, a prostate cancer diagnosis may only be made with absolute certainty with an image-guided prostate biopsy. The biopsy samples taken during the process are graded for cell differentiation and cancerous aggressiveness using the primary, secondary, and total Gleason scores (Fig. 1B). Patients may be defined as having clinically significant malignancy if their specimens have a higher histopathological Gleason score (usually total Gleason score 7 or primary Gleason score 4). On the other hand, a clinically inconsequential tumor is one that is localized to one organ, has a low-grade histology (a total Gleason score of 6 with no Gleason component 4), and has a gross tumor volume of 0.5 cc. [5]

Alternatives for treating prostate cancer. Those who have been diagnosed with clinically significant PCa may choose to treat it with radical prostatectomy (RP), whole-gland radiation therapy (RT), or hormonal therapy. Urinary incontinence and impotence are two undesirable side effects that some patients with terminal illnesses may experience as a result of therapeutic therapy. Serum PSA levels, imaging, and rebiopsy can be used together to detect disease recurrence, if any, after treatment. Active surveillance or watchful waiting programmes are commonly used to track low-risk or clinically inconsequential diseases. These programmes may involve imaging to track disease progression and/or serial biopsies to look for changes over time. Treatment options for localized PCa are constantly evolving, and recent research suggests that image-guided focused therapy or male lumpectomy may become increasingly common in the near future.

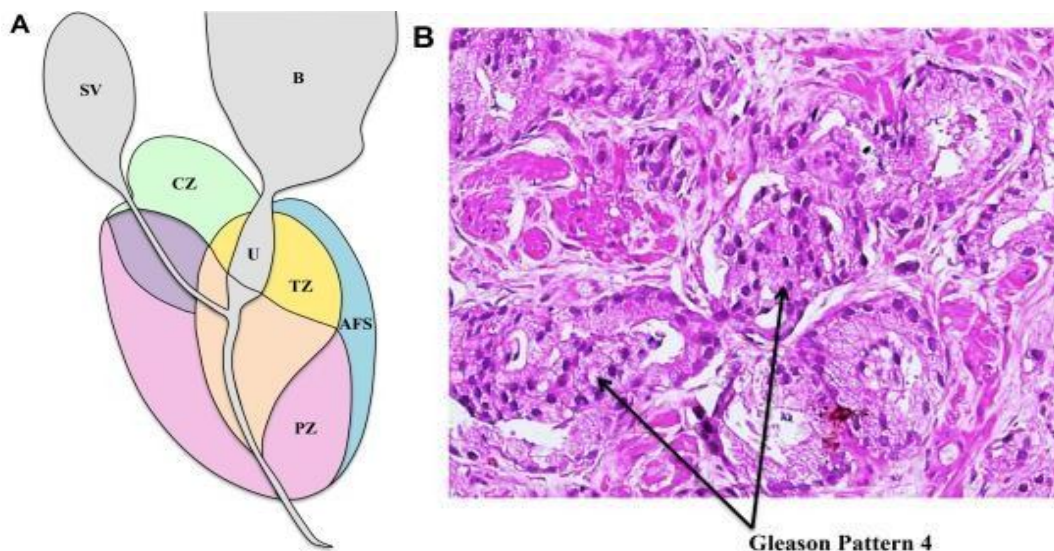


Figure -1: (A) Prostate zonal anatomy is depicted with the McNeal zones in sagittal view. SV: seminal vesicle (gray), B: bladder (gray), CZ: central zone (green), U: urethra (gray), TZ: transition zone (yellow), AFS: anterior fibromuscular stroma (blue), and PZ: peripheral zone (pink) (B) Immunostained biopsy specimen demonstrating Gleason pattern 4 adenocarcinoma of the prostate.

2. IMAGING MODALITIES

For the detection and localization of PCa, imaging has recently become the standard. US-based imaging, mpMRI, mpMRI-US fusion imaging, and PET imaging are the current leading modalities for image-guided diagnosis of PCa. The underlying tumor's biological behavior will determine the imaging mode of choice. As shown in Figure 2, we summarize how the characteristics of the tumor observed correlate to the imaging modalities used. In the parts that follow, we'll also dive deeper into each of the specific correspondences. Table 1 summarizes the main imaging modalities, including their primary therapeutic applications as well as their pros and limitations.

US based Imaging.

When it comes to imaging PCa, anatomical ultrasound imaging has been around the longest and is still the gold standard. Functional imaging techniques developed in the United States have recently piqued the curiosity of the scientific community. We examine the many US imaging approaches that are currently leading to the creation of an mpUS-based approach for PCa detection in the sections that follow.

B-mode or grayscale U.S. The most common imaging method for detecting PCa is grayscale or standard B-mode US. B-mode US is useful for distinguishing the zonal architecture of the prostate, with the outside PZ appearing more echogenic than the interior CZ and TZ. Grayscale transrectal ultrasonography (TRUS) imaging was first used by Hodge et al. to guide six biopsy needles into the prostate in 1989. Since then, random and systematic prostate biopsies have been the gold standard for detecting PCa, and this method has served as its foundation, along with the additional targeting of hypoechoic lesions (cancer tissue with cellular architecture defects appears less echogenic than normal tissue on grayscale US, as shown in Fig. 3). [6,7] An extended sextant 12-core biopsy, aiming for the apical and lateral parts of the PZ where the cancer is most likely to be hiding, has been the subject of numerous discussions on how to maximize its likelihood of detecting cancer. [8]

The use of traditional B-mode anatomic US imaging for PCa has various drawbacks. Prostatitis, inflammation, and benign prostatic hyperplasia (BPH) can all make the prostate appear hypoechoic on US imaging, just like cancerous cells. In addition, early-stage carcinomas can have an isoechoic appearance as compared to later stages because of the greater amount of normal glandular tissue present at that time. Up to 60% of morphologically worrisome lesions in the United States are known to be benign, while 21%-47% of tumors may be missed on an initial biopsy. [9-10] Since random and systematic sampling schemes are not tumor or patient specific, they can result in the unintentional detection of clinically insignificant PCa (low-volume cancer with a total Gleason score 7)[11-12] and the undergrading of the disease's aggressiveness due to insufficient sampling of the bulk of the tumor. [13]

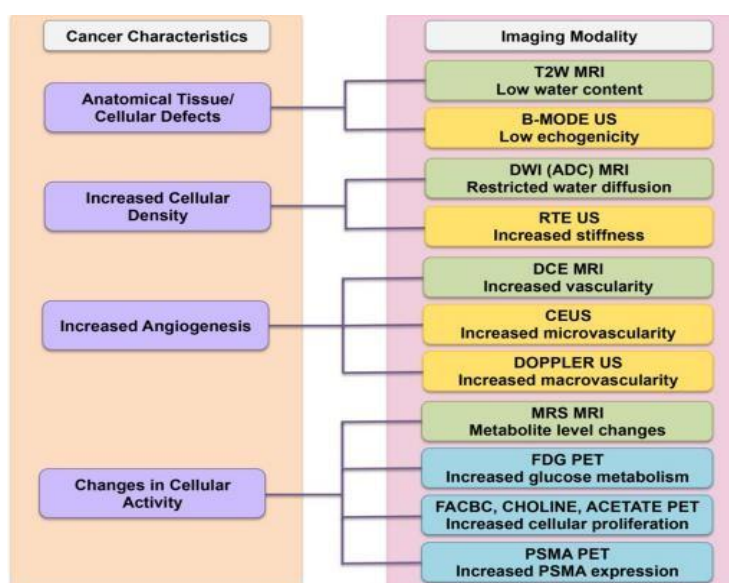


Figure 2. Correspondence of imaging modality to cancer characteristics. The left column shows the biological cancer characteristics and their correspondence to the choice of imaging modalities

Table 1. A summary of clinical usage, advantages, and disadvantages across imaging modalities for PCa imaging.

IMAGING MODALITY	CLINICAL USAGE	ADVANTAGES	DISADVANTAGES	FUTURE
ultrasound-based	initial detection and diagnosis	Office-based, widely available, inexpensive, real-time imaging	limited tissue contrast between cancerous and benign tissue	mpuS-based approach (rte, ceuS) may improve contrast
mpmri-based	initial diagnosis and recurrence, active	excellent tissue contrast for identification of	expensive due to in-bore time, lack of real-time imaging, requires advanced	alternative in-bore options with real-time imaging being
	surveillance, staging, metastatic involvement	clinically significant PCa	training	developed
mpmri- ultrasound fusion-based	initial detection and diagnosis, active surveillance	Office-based, combines multimodality information	relatively costly, requires either fusion-device specific training or ample experience to perform cognitive fusion, registration errors during mri- ultrasound fusion	gaining popularity globally, but further improvements to minimize registration errors needed
pet-based	Staging, recurrence, metastatic spread	offers ancillary information for tumor staging, characterization and metastatic involvement	expensive, technological (e.g. attenuation correction) and/or clinical challenges (e.g. radiation exposure)	development of specific radionuclides is an ongoing endeavor

US picture analysis with the help of a computer. Alterations to cell structure are a hallmark of PCa, and these alterations influence the way US signals backscatter. This information can be utilized to distinguish between cancerous and normal tissue. Several products on the market perform real-time, computer-based analysis of these US signals; for instance, one can use statistical analysis of raw US data to create a prostate histogram (Prostate HistoScanning [PHS]), while another can use an artificial neural network to analyze digital B-mode ultrasound images (ANNA/computerized transrectal ultrasound [CTRUS]).



Fig - 3 B-mode US image of the prostate depicting hypoechoic lesion (red oval).

Prostate HistoScanning. PHS is a method for identifying potentially malignant prostate lesions through statistical analysis of raw backscattered US. Early research by Braeckman et al. on 29 patients undergoing RP demonstrated a sensitivity of 100%, specificity of 82%, NPV of 80%, and PPV of 100% for lesions more than 0.5 mL in volume. [14] Twenty-seven patients were analyzed in a study by Simmons et al., who found that PHS had a sensitivity of 90% and a specificity of 72% for lesions at least 0.2 mL in size. PHS functioned poorly in the front prostate and optimally in the central and posterior halves of the gland. [15] The detection of lesions 0.1 cm³ in 98 men was shown to have a sensitivity of 60% and a specificity of 66% by Macek et al. [17] Despite Javed et al.'s efforts, PHS has been shown to be unreliable in typical clinical settings across three separate investigations involving a total of 105 men. In these investigations, PHS was used to evaluate patients before they had RP (n = 24), TTB (n = 57), or a transperineal template biopsy (TGB; n = 24). Cancer was found at a higher rate in PHS (38.1%) than in TGB (62.5%) and TTB (13.4% vs. 54.4%). Furthermore, PHS and RP pathology yielded inconsistent results when comparing tumor volume estimates. For 148 patients, Schiffman et al. also discovered no connection between RP and PHS tumor volumes. However, at present, the reliability of this method for PCa detection is compromised by a lack of strong, consistent clinical data. [16]

The use of transrectal ultrasound imaging and artificial neural networks. Classifying tissue areas as malignant or benign using ANNA of C-TRUS images is at the heart of the ANNA/C-TRUS system for PCa detection. The doctor performs a standard B-mode transrectal US exam of the prostate, sends the digital images to a central server, and receives them back with potentially cancerous spots highlighted. The user is then able to direct biopsies to the selected areas. To train the ANNA classifier, we used sets of correlated US images from RP specimens annotated with pathological information. Half of the 132 men studied who had one to seven negative conventional grayscale US biopsies were found to have cancer by the ANNA/C-TRUS method. Conventional US-guided systematic approaches have a historical detection rate of 7% for PCa in males with repeat biopsy. [17] Another research of 75 biopsy-naïve men found that 41% of them had PCa, which was detected by the ANNA/C-TRUS. Strunk et al. showed that using mpMRI in conjunction with C-TRUS enhanced the identification of PCa in high-risk individuals. Larger multi-center trials are required to gauge the true therapeutic efficacy of ANNA/C-TRUS, which has shown encouraging initial results.

Doppler US. Over-vascularization and new blood vessel growth are common features of PCa. When US waves from a transducer hit the moving red blood cells in the blood vessels, the reflected waves alter in frequency in a manner that is proportionate to the cells' velocities, as demonstrated by the Doppler effect. Changes in frequency are color-overlaid on real-time B-mode US images to show areas of enhanced perfusion, such as those seen in tumors. The core of PCa detection using color Doppler ultrasound (CDU) imaging is focusing on these areas of enhanced blood flow. Another variation, known as power Doppler ultrasonography (PDU), visualizes the total integrated Doppler power in color. PDU imaging is more sensitive to perfusion than CDU, and hence may be better able to detect reduced blood flow in smaller diameter blood arteries, but at the cost of losing the sensation of flow direction. When it comes to detecting PCa, Doppler imaging has mixed results. There was no advantage to employing Doppler imaging for PCa detection in a study of 62 patients that compared high-frequency CDU and PDU to random sextant biopsy. [18] Okihara et al. used PDU imaging to examine 107 males with elevated serum PSA levels. The ultimate sensitivity, specificity, PPV, and NPV for PDU imaging indicating a lesion were 98%, 78%, 59%, and 99%, respectively. In a study including 243 males, Sauvain et al. demonstrated that PDU imaging has a sensitivity and specificity of 45% and 74%, respectively, for diagnosing low-risk PCa. [19] Doppler US imaging for PCa detection is restricted by its inability to detect blood flow in capillaries smaller than 0.1 mm⁹. Neo-microvessels, which range in size from 10-50 μm on average, proliferate at an accelerated rate during cancer development. Doppler imaging may only be useful for detecting cancers with advanced stages and high Gleason grades since it can only detect increased blood flow in larger macrovessels.

Ultrasound imaging with contrast medium. Angiogenesis and disordered neovascularization, which can greatly increase microvascular density (MVD), are frequently observed alongside tumor growth and progression within the prostate. Contrast-enhanced ultrasound (CEUS) imaging aims to detect this improvement in MVD. During a biopsy with CEUS imaging, microbubbles loaded with a highly echogenic gas are injected intravenously. These microbubbles are the same size as red blood cells, so they may travel through (and be imaged by) the tiny blood vessels that supply tumors. CEUS has this advantage over Doppler US imaging, which can only focus on the flow in bigger macrovessels due to its lower resolution. Asymmetrical fast or focused enhancement is typically used to identify malignancy using CEUS. CEUS quantitative analysis can be performed by tracking the concentration of the US contrast agent over time or by computing the agent's dispersion kinetics as it travels through the microvasculature. [20] Li et al. conducted a meta-analysis of 16 studies involving 2624 patients and concluded that CEUS imaging has a combined sensitivity and specificity of 70% and 74%, respectively, for the identification of PCa.

Real-time elastography. It's common knowledge that PCa tissue is more rigid than regular prostate tissue. Increased stiffness of malignant tissue in the prostate is caused by the increased cellularity, increased micro vascularity, loss of glandular architecture, reduction in acinar area, and increased collagen deposition in the stroma around cancer. [21] Actually, the physical DRE relies on the clinician utilizing his or her index finger to palpate the posterior PZ of the prostate in order to discover firmer or stiffer aberrant masses of cancer tissue. Real-time elastography (RTE) is an improved and more trustworthy whole-gland option for finding these stiffer regions within the prostate gland. Mechanical stimulation of the prostate tissue is induced by the physician, and the resulting response is imaged, typically with real-time US, in RTE imaging. Strain elastography (SE), acoustic radiation force impulse (ARFI) imaging, and shear wave elastography are all examples of techniques that can be categorized according to the excitation method (SWE).

Strain elastography. A US probe is used to mechanically compress and release the prostate tissue repeatedly in SE. Differential strain or deformation of the prostate tissue is generated, and it is shown as a color map superimposed on real-time B-mode US pictures. The live color map helps distinguish stiffer tissue from softer tissue and enables the clinician to guide the biopsy needle to the stiffer areas (and hence more likely to be malignant) in the prostate. In a meta-analysis, Zhang et al. looked at seven studies that compared the accuracy of diagnostic SE with RP specimens as gold standards. Overall, the pooled sensitivity and specificity in this sample of 508 males was 72 and 76 percent, respectively. [22] Comparisons between SE and MRI-guided biopsies have also been made. In their study of 33 patients with PZ lesions, Aigner et al. found that strain RTE and T2-weighted MRI had identical sensitivity and NPV. Fifty patients with biopsy-proven malignancy who underwent strain RTE and mpMRI exams to identify PCa were evaluated in a retrospective research by Pelzer et al. There was a relationship between the outcomes and RP samples. Although the authors noted that the MRI findings may have been biased by the prior biopsies that generate hemorrhage abnormalities on MRI, the sensitivity of strain RTE was greater than mpMRI (92% vs. 84%). Interestingly, MRI worked better in the base and TZ, while strain RTE did better in the dorsal and apical to middle regions of the prostate. By fusing MRI and strain RTE to pinpoint worrisome tumors, Brock et al. increased specificity in a population of 121 previously negative men receiving fusion biopsies. For MRI/strain RTE fusion, the sensitivity and specificity were 77.8% and 77.3%, respectively, compared to 74.1% and 62.9% for MRI alone. Free-hand compressions and decompressions with the endorectal US probe pose a significant challenge to SE because they rely heavily on the skill of the operator. To counter this, Tsutsumi et al. looked explored employing inflated balloons for applying more uniform compressions. The difficulty of SE is compounded by the fact that the live color mappings are subjective to each individual operator. The color maps are automatically scaled to the maximum and lowest strains in a specific 2D imaging plane, and it is tough to establish an absolute quantitative 3D threshold of stiffness that can discriminate malignant from benign tissue in the entire gland.

Impulse imaging using acoustic radiation force The prostate tissue is imaged using ultrashort (1 millisecond) focused US beams of high intensity during ARFI imaging. Tissue is displaced due to an acoustic radiation force generated when momentum is transferred from the acoustic US waves to the propagating medium. Next, the US inquiry measures the resulting shift. It's the same principle as with strain imaging: tumors and other stiffer parts of the prostate will cause less displacement than healthy tissue. By displaying a color-coded map of displacements in real-time, the doctor can biopsy these areas with pinpoint accuracy. ARFI's key benefit over SE is that it does not require skilled manual compressions and decompressions of the prostate. On nine human prostate specimens, Zhai et al. [23] used ARFI imaging to differentiate between McNeal zones, BPH, calcifications, atrophy, and malignant tumors. An in vivo study involving 19 individuals before prostatectomy confirmed these findings. In both trials, however, the restricted depth penetration of the ARFI pulses hampered the detection of anterior PCa.

Shear wave elastography. In SWE, a shear wave is produced in the prostate by means of acoustic radiation force, and its velocity is subsequently measured. Since the Young's modulus (a measure of tissue stiffness reported in kPa) is inversely related to the shear wave velocity, SWE can be used to generate a quantitative image of tissue stiffness. SWE imaging, in contrast to SE, does not necessitate manually pressing the probe, and it is quantitative as well. These two features make SWE more transferable and less dependent on the skill of the user. A sensitivity of 96%, specificity of 96%, PPV of 69%, and NPV of 100% were obtained in an initial SWE evaluation study of 53 males utilizing a Young's modulus threshold of 37 kPa to distinguish benign from malignant tissue. Using a threshold of 35 kPa, Correas et al. found a sensitivity, specificity, PPV, and NPV of 96%, 85%, 48%, and 99%, respectively, in a real-time SWE research including 1040 PZ sextants in 184 men. For 60 patients, Boehm et al. used whole-gland SWE to determine a threshold of 50 kPa before performing a prostatectomy. They found an 81% sensitivity, 69% specificity, 67% PPV, and 82% NPV. [24] In a research of 50 men, Ahmad et al. found a correlation between rising Young's modulus and rising Gleason grade, with a sensitivity and specificity of around 90% for both. However, unlike previous investigations, this one found significantly different absolute stiffness levels between benign and malignant tissue (75 kPa vs. 134 kPa, respectively). First results from SWE imaging have been promising and multiple

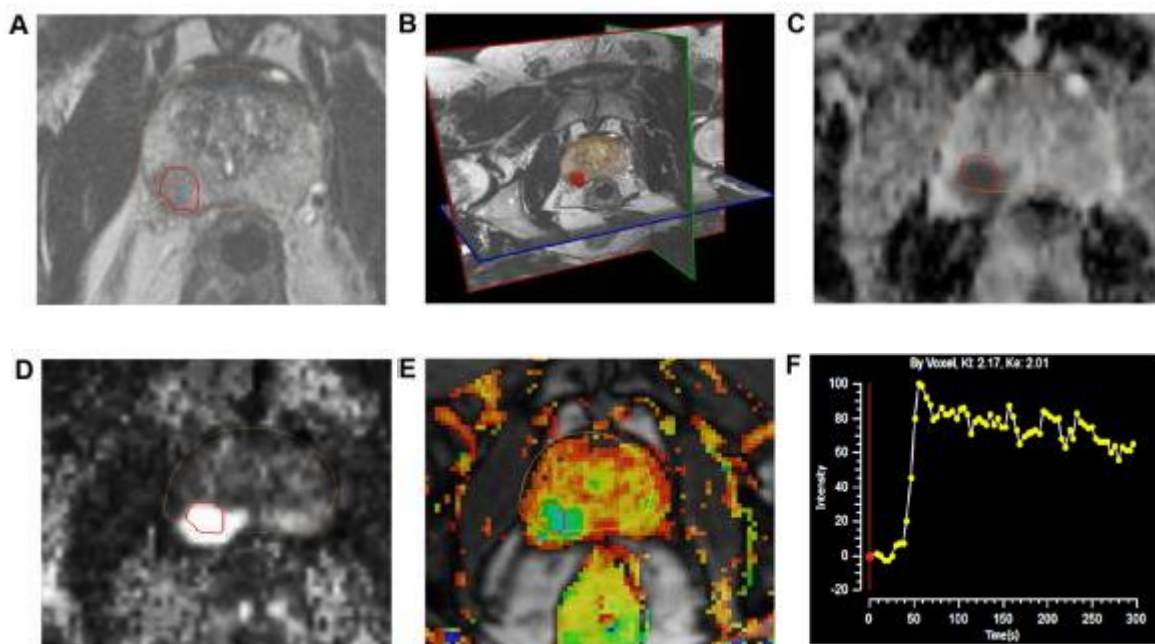
investigations have indicated that there is a considerable difference between the Young's modulus of benign and cancerous tissue. However, a hard numerical cutoff between the two has yet to be established.

Multiparametric US. All US-based imaging approaches leverage tumor biology properties including increased vasculature, stiffness, etc. Researchers have recently used mpUS to improve targeting specificity by combining these functional methods. Aigner et al. sampled five targeted cores in 133 men using RTE and CEUS. Biparametric detection yielded 59.4% cancer detection. In 150 men, Xie et al. used grayscale, Doppler, and CEUS imaging to identify 49%. mpUS recognized more PCa patients than grayscale, power Doppler, and grayscale plus power Doppler ($P = 0.002, 0.001, \text{ and } 0.031$, respectively). Brock et al. evaluated RTE and CEUS pathology in 86 patients with whole-mount sections. RTE and CEUS reduced false positives from 35% to 10% and boosted PPV from 65% to 90%. mpUS has shown early promise, but multicenter trials with bigger patient cohorts are needed to develop it.

MMRI.

MRI for PCa detection has used a multiparametric approach, unlike US-based methods. Anatomical sequences (T2-weighted MRI) are paired with at least two functional sequences (DWI and dynamic contrast-enhanced imaging) to image the tumor's biological features. MR spectroscopy, another functional MRI method, may be included in the acquisition protocol for facilities with expertise. These imaging methods, called mpMRI, provide simultaneous tumor

T2-weighted imaging assessment. High-resolution axial, sagittal, and coronal T2-weighted imaging (T2WI) sequences show prostate zonal anatomy and soft tissue contrast (Fig. 4B). T2WI can best detect zonal anatomical anomalies in PCa cells (or to depict seminal vesicle invasion and extracapsular extension of disease). Normal PZ tissue is water-rich with many ductal and acinar components and sparsely interlaced smooth muscle. T2-weighted pictures show it as bright. PCa in the PZ shows as a rounded or ill-defined low-signal intensity focus (Fig. 4A), unlike the loosely packed typical PZ tissue. Prostatitis, atrophy, and previous biopsy-related haemorrhages can mimic a low-signal intensity focus in the PZ of T2-weighted images. On T2WI, normal TZ tissue looks darker than the PZ due to its lower water content, compact smooth muscle, and sparser glandular components. PCa in the TZ appears as a uniform, low-signal mass with fuzzy borders. Due to its large muscle and fibrous content, the TZ may look low-signal intensity, making it difficult to identify cancer from stromal BPH. [24] DWI. PCa has dense tumor cell areas. The high intracellular/extracellular volume ratio of these locations limits water molecule Brownian motion in the extracellular space. DWI detects water molecules' random Brownian motion. Changing magnetic field duration and strength yields two or more DWI pictures (indicated by a b-value). Cancer appears bright hyperintense on DW imaging because restricted water diffusion reduces signal loss. Cancers appear as hypointense dark spots on an Apparent Diffusion Coefficient (ADC) map made from numerous b-value DW images (Fig. 4C). ADC readings predict cancer aggressiveness. Ultra-high b-value DWI (e.g., 2000 seconds/mm²; Fig. 4D) may improve index lesion determination.



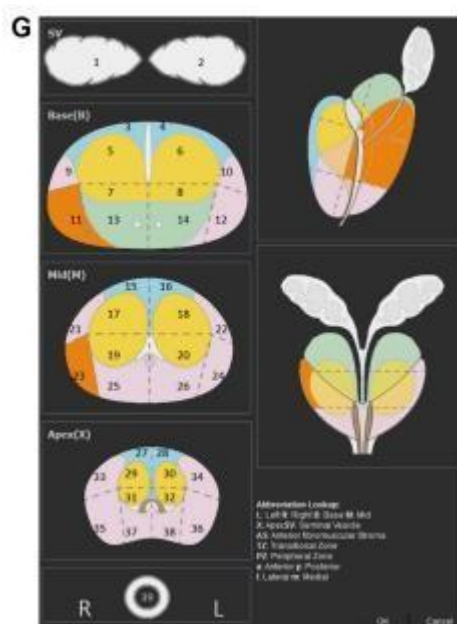


Fig - 4 : The mpMRI depiction of right posterolateral lesion: (A) axial T2-weighted image with lesion in red outline, (B) 3D T2-weighted view of prostate contour (brown) and lesion (red), (C) ADC image with lesion in red outline, (D) computed high b-value = 2000 seconds/mm² image with lesion in red outline, (E) dynamic contrast-enhanced pharmacokinetic map with lesion in red outline, (F) average time-signal intensity curve plot of the lesion, and (G) PIRADS version 2 location of lesion (orange).

Dynamic contrast-enhanced imaging. DCE-MRI uses 3D T1-weighted images before, during, and after intravenous contrast media injection (typically low-molecular-weight Gadolinium chelates that rapidly diffuse in extravascular extracellular space). As said, aggressive tumors produce angiogenic agents that stimulate microvessel proliferation. New microvessels are disordered and leaky due to weakened walls. Tumor angiogenesis causes early DCE-MR enhancement in PCa tissue. The DCE-MR images are usually analyzed for lesions (a) qualitatively, by visual inspection of subtraction time points for potentially cancerous spots showing focal enhancement; (b) semi quantitatively, by time-signal intensity curve analysis (Fig. 4F) of suspicious voxels to determine parameters like time-to-peak, wash-in slope, etc.; and/or (c) quantitatively, by compartmental pharmacokinetic modelling that uses contrast media concentration and other parameters (Fig. 4E).

Magnetic resonance spectroscopic imaging. MRSI measures prostate tissue cellular metabolite concentrations. Citrate is high in healthy prostate tissue, especially in the PZ. Cancerous tissue lowers them. PCa also increases choline levels due to cell density, cell membrane turnover, and phospholipid metabolism. MR spectroscopy distinguishes PCa tissue by its high choline-to-citrate ratio. Because creatine and choline have similar resonant peaks, the ratio of choline + creatine to citrate is usually employed. Turkbey et al. found that MRSI enhances mpMRI-based PCa detection. [25] MRSI takes longer and demands technological skill. Its clinical use for PCa diagnosis is limited. It generally stages and detects radiation recurrence.

mpMRI-detected PCa. mpMRI-based PCa detection is successful. Rais-Bahrami et al. discovered that biparametric MRI (T2WI + DWI) had an AUC of 0.8 for PCa detection in 143 men (which outperformed the AUCs of 0.66 and 0.74 for PSA level and PSA density, respectively). Schoots et al. meta-analyzed the diagnostic benefits of mpMRI-targeted biopsies compared. systematic biopsies. MRI-guided biopsies detected clinically significant cancer (91% vs. 76%) and clinically insignificant cancer (44% vs. 83%) better than TGBs. Panebianco et al. randomly assigned 1140 males to either standard TGBs or mpMRI + TGBs. The first cohort detected 38% and the second 72%. No men with negative MRIs developed clinically significant cancer on saturation biopsies. Targeting MRI-suspicious lesions is beneficial for biopsy-naïve, previous negative, and active surveillance patients. The scanning acquisition procedure and scan reading accuracy are crucial to mpMRI-based PCa detection. Standardizing prostate mpMR imaging acquisition and reading is underway. The European Society of Urogenital Radiology (ESUR) published the Prostate Imaging and Reporting Data System (PIRADS) in 2012 to standardize mpMRI lesion acquisition and cancer suspicion level and site assessment. PCa detection increases with PIRADS suspicion level in several trials. Recently, the

American College of Radiology, ESUR, and AdMeTech foundation worked to upgrade this standard to PIRADS version 2, which among other changes also promotes the use of 39-region charts (Fig. 4G) to define lesion locations. According to the newest PIRADS version 2, DCE-MRI does not help to the overall assessment of suspicion level for lower grade (PIRADS levels 1 and 2) and higher grade lesions (PIRADS 4 or 5). (PIRADS 4 or 5). A positive DCE-MRI raises PIRADS level 4 suspicion for equivocal or moderate-grade PIRADS 3 lesions. Hence, the mainstream expert opinion currently considers diagnostic quality T2WI and DWI/ADC images to be the major MRI sequences used for suspicion level assessment of lesions. DCE-MRI is still suggested to detect tiny clinically important tumors.

MRI-US fusion.

This section discusses a new PCa imaging method that combines US and MRI. Fusion imaging combines the advantages of US and MR imaging without compromising their diagnostic clinical relevance. mpMRI's clinically substantial PCa detection sensitivity and specificity have transformed PCa diagnosis. Hambroek et al. compared in-bore mpMRI-guided biopsies to 10-core systematic TRUS biopsies in men before RP. MRI-guided biopsies detected PCa 88% better than grayscale TGBs (55%; P-value 0.001). MRI is accurate, but given the number of prostate biopsies conducted each year, it is too expensive and impractical to utilize alone (approximately a million in the US alone). In-bore biopsies take longer without real-time imaging, making patients uncomfortable. Due to the intense magnetic field, safety requires specialist equipment and needles. In-bore biopsies with real-time imaging and faster robotic needle placements are being developed. [26-27] Grayscale US imaging is cheaper and faster than in-bore MRI, although it may not be as diagnostic. mpMRI-US fusion-guided biopsies are now a feasible alternative to MRI-guided, in-bore, and conventional TGBs. MRI-US fusion-guided biopsies are conducted in an outpatient clinic with live B-mode US, reducing expenses and treatment time. To identify aberrant MRI areas, the patient undergoes an mpMRI pelvic examination before the operation. The biopsy procedure targets these sites by mapping them onto US images via image fusion or registration. Expert urologists can cognitively or visually fuse MRI and US pictures. This is subjective and may require knowledge only found in huge academic research institutions. Regulatory-cleared, commercially available MRI-US fusion devices are growing more popular. Real-time US biopsies of virtual MRI targets are easier with fusion platforms. The platforms differ in US capture (3D volumetric, 2D sweep, etc.), biopsy targeting (e.g., electromagnetic and electromechanical), biopsy route (transrectal vs. transperineal), and image fusion technique (rigid vs. elastic). Most systems store biopsied sites with abnormal grading and use MRI/US fusion-based targeting guidance. Active surveillance and targeted therapy depend on accurate biopsy placements; therefore, this has major implications for patients. Three widely investigated fusion biopsy platforms—Artemis (Eigen), UroNav (Invivo/Philips), and Urostation—will be discussed here (Koelis). BiopSee, Virtual Navigator, HI RVS, BioJet, Mona Lisa, and LOGIQ 9 (MedCom, Esaote, Hitachi, and GeoScan) are other platforms (GE Healthcare).

Artemis. Eigen, USA, makes Artemis. Semirobotic mechanical stability of the TRUS probe during biopsy reduces free-hand distortion. ProFuse radiology software annotates worrisome lesions in 3D mpMR images before the surgery. The TRUS probe mechanically rotates to acquire 3D volumetric US data. This 3D US volume is rigidly and elastically merged with the 3D MRI volume (Fig. 5A and 5B). Rigid fusion corrects orientation variations between 3D MRI and 3D US volumes, while elastic fusion accounts for local shape deformations caused by patient orientation, bladder/rectal filling, and endorectal coil or TRUS probe pressure. Fusion transfers virtual MRI lesion sites to real-time TRUS images for targeting. After fusion, a visible graphical interface based on electromechanical tracking and shot sites moves the probe/needle guide assembly to lesion spots (Fig. 5C). MRI-US fusion-based targeting and automatic template distribution of systematic, random biopsy cores based on prostate form and volume are available. The Artemis system revealed cancer in 53% of a mixed group of 171 men on active surveillance and earlier negative biopsies in a Sonn et al. investigation. Fusion biopsy-guided cores detected three times more malignancy than systematic random biopsies and more clinically relevant tumors ($P = 0.001$). The biopsy findings corresponded with mpMRI suspicion level of the targeted lesions, and men with the highest suspicion level had a 94% cancer detection rate. [28] Sonn et al. revealed 34% of prior negative men got PCa, 72% of whom had clinically severe illness. Fusion biopsies found 1.4 times but 15% as many unimportant tumors, according to Sonn et al. Wysock et al. compared Artemis-targeted and expert cognitive fusion biopsies in 125 men with 172 MRI-suspicious lesions. Artemistargeted fusion biopsies found 20.3% clinically significant tumors per target compared to 15.1% utilizing cognitive targeting ($P = 0.0523$). Device-targeted biopsy was more pathologically informative than cognitive biopsies ($P = 0.0104$).



Fig - 5: Depiction of MRI-US fusion. (A) and (B) show axial slices of fused MR and US images, (C) 3D prostate surface (brown) with archived biopsy core locations (white cylinders) after systematic and fusion biopsy

UroNav. Invivo/Philips markets the UroNav platform, created at the National Institutes of Health, Bethesda, USA. An external electromagnetic field generator tracks and guides needle biopsies transrectally. DynaCAD for Prostate marks problematic lesions on preprocessed 3D mpMR images. A 2D freehand sweep from prostate base to apex acquires the 3D US volume during biopsy. A stiff method that accounts for rotational and translational variances can fuse 3D MRI and 3D US pictures. Visually adjusting the US probe pressure on the prostate can change the distortion between the US and MR 3D pictures. After fusion, electromagnetic guidance guides the probe/needle assembly to virtual MRI lesions. Pinto et al. discovered PCa in 28%, 69%, and 90% of 101 patients using the UroNav platform ($P < 0.0001$). In their investigation, the number of mpMRI sequences (T2WI, DCE, DWI, and MRSI) that detected a lesion as positive—low (2 or less), moderate (3), or high (4)—determined its suspicion grade and the chance of cancer upon biopsy. Vourganti et al. found PCa in 37% of 195 men with prior negative biopsies, and fusion-guided biopsies found high-grade malignancy in all males ($n = 21$), while systematic biopsies missed them in 12 individuals. [29] Siddiqui et al. discovered that targeted biopsy revealed 30% more high-risk cancer ($P < 0.001$) and 17% fewer low-risk cancer ($P < 0.001$). Targeted biopsies outperformed systematic biopsies in predicting low-risk cancer in 170 men following RP ($P < 0.05$).

Urostation. Koelis, France's Urostation platform uses software image registration instead of electromechanical or electromagnetic tracking like Artemis and UroNav. A 3D US probe stitches together an initial volume. This 3D volume marks consecutive biopsy spots. The US volume is elastically merged with 3D MR images to map MRI lesions. Then, the US probe is freehand-manoeuvred to the lesion areas for biopsy. A 3D volume is taken with the needle in place and elastically fused with the initial 3D reference volume to confirm each biopsy location. Using fusion-guided biopsy, Ukimura et al. targeted MR-visible, hypoechoic, and isoechoic lesions on a phantom with the Urostation platform. 84% of fusion-guided biopsies hit lesions. In a retrospective investigation of 90 patients, Rud et al found PCa diagnosis rates of 10%, 27%, and 91% for low-, medium-, and high-MRI suspicion levels. Fusion biopsies detected more clinically serious cancer in 152 men than systematic biopsies ($P = 0.03$).

PET Imaging. Gamma cameras image intravenous radiolabeled tracers in the prostate during PET. It is utilized for cancer staging, biochemical failure following radiation, and lymph node metastases (Fig. 6). PET/MRI or PET/CT is utilized with anatomical imaging to show prostate cell metabolic, molecular, or cellular activity. The tracer and biological process (metabolism, cellular growth, receptor binding) determine PET imaging modalities.

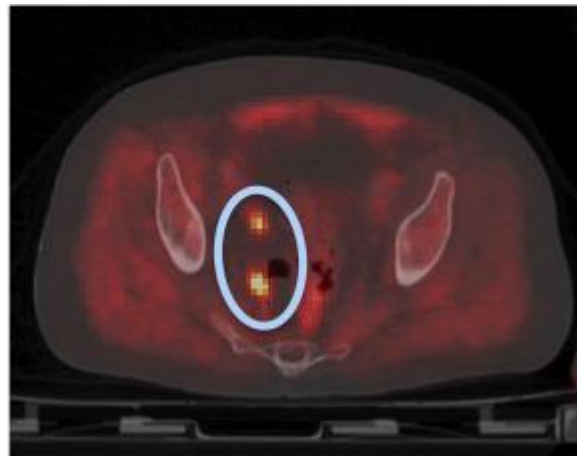


Fig – 6: PET/CT image postprostatectomy depicting possible lymph node metastasis (blue oval with orange hot spots)

Metabolism-focused. 18F-fluorodeoxyglucose. The Warburg impact leading the change glycolytic pathway glucose metabolism in malignant tissue than normal tissue. 18F-fluorodeoxyglucose is the most common tumor glucose metabolism radiotracer (18F-FDG). 18F-FDG cannot detect early or recurring PCa due to inadequate glucose metabolism in small, developing PCa cells and the prostate's close proximity to the urine bladder, which confounds uptake data. Tumor cells with inadequate glucose metabolism have low radiotracer uptake and overlap with normal tissue and BPH. Prostatitis may ingest more FDG than PCa cells. Yang et al. studied 100 patients with incidental FDG uptake and found that 20 had malignant lesions and 80 had benign lesions. In PSA recurrence patients with negative whole-body bone scans, FDGPET imaging may still reveal pelvic lymph node metastases. In an early investigation of 24 men with negative bone scans, Chang et al. reported FDG-PET imaging to have 75% sensitivity, 100% specificity, 100% PPV, and 67.7% NPV for detecting metastatic pelvic lymph nodes.

Proliferation. 1-Amino-3-fluorine-18-fluorocyclobutane-1-carboxylic acid. PCa cells upregulate amino acid transport, which the radiotracer 18-F ACBC exploits. This radiotracer's low urinary excretion improves 18-F ACBC uptake detection in malignant tumor cells. [30] Schuster et al. found that 18-F ACBC PET detected recurrent prostate cancer more sensitively (89%) than FDA-approved [¹¹¹In]capromab pendetide SPECT/CT or ProstaScint (69%). Schuster et al. additionally found that the highest standardized absorption value of anti-18-F ACBC associated with Gleason score at all time points ($P < 0.05$) in PCa prostatectomy specimens. [31] Turkbey et al. examined 21 patients before prostatectomy with 18-F ACBC PET/CT and 3T mpMR. 18-F ACBC PET/CT demonstrated a sensitivity of 90% for dominant PCa and 67% and 66% for PCa, respectively, compared to histopathologic results. BPH overlapped with cancer tissue's increased tracer uptake. T2-weighted MRI with 18-F ACBC had a tumor localization PPV of 82%, greater than either modality alone. 11C-Choline, 18F-fluorocholine. PCa increases membrane production. Choline transporters bring choline into cells to synthesize phosphatidylcholine, a cell membrane component. Index cancers ingest 11C-choline and 18F-fluorocholine (FCH) radionuclides for tracer imaging. Kwee et al. performed FCH PET/CT in 50 patients with increased PSA levels after treatment (RP, RT, brachytherapy). 88% of patients with a PSA < 1.1 ng/mL had abnormal tumor uptake, compared to 6% below this threshold. Thus, imaging PSA levels affected FCH PET/CT's to identify PCa recurrence. Simone et al. assessed biochemical recurrence in 146 patients with low PSA (< 1 ng/mL) using a new FCH PET/CT imaging acquisition strategy with an early dynamic phase. In this low PSA cohort, FCH PET/CT had a sensitivity of 79%, suggesting it could detect PCa recurrence early. [Kitajima et al. compared 11C-choline PET/CT to mpMRI in 115 prostatectomy patients. mpMRI outperformed 11C-choline PET/CT for recurrence diagnosis (AUC 0.909 vs. 0.761, P-value 0.01). However, 11C-choline PET/CT outperformed mpMRI for lymph node metastatic identification. A meta-analysis of 3167 individuals from 47 studies found 11C-choline or 18F-FCH PET/CT beneficial as a first imaging scan for PCa patients with biochemical recurrence and PSA values between 1 and 50 ng/mL.

Receptor-targeted. PSMA. PSMA is a membrane glycoprotein having a large extracellular, transmembrane, and intracellular domain. All stages of PCa substantially upregulate prostatic epithelial cell PSMA. [32] PSMA expression increases with tumor aggressiveness, metastasis, and disease recurrence, making it a rational target for ligand- receptor-based imaging and therapy. Radiolabeled antibodies/antibody fragments have targeted intracellular or extracellular antigen motifs in animal

models and pilot human trials. ⁶⁴Cu-labeled aptamers and ¹¹C-, ¹⁸F-, ⁶⁸Ga-, and ⁸⁶Y-labeled low-molecular-weight PSMA inhibitors are PSMA-based radiotracers. In initial clinical trials, ⁶⁸Gal- labeled PSMA inhibitor detected PCa relapse and metastases better than ¹⁸F-choline. [33] Indium-111 radiolabeling of the 7E11C5.3 antibody produced ProstaScint scan, the only FDA-approved PSMA agent. ProstaScint scan can describe recurrence in patients with increased serum PSA levels following primary therapy by identifying the intracellular part of PSMA. Preoperative lymph node staging using ⁶⁸Ga-PSMA-PET outperformed CT and MRI in 130 intermediate- to high-risk PCa patients. Ga-PSMA has also been demonstrated to restage PCa in salvage RT candidates with PSA levels <0.5 ng/mL.

3. DISCUSSION

Hodge et al. pioneered prostate transrectal biopsies using grayscale B-mode US imaging in 1989. Transrectal US swiftly replaced physical DRE for guiding needle biopsies for PCa diagnosis. Today, imaging is essential for PCa management. US, MRI, and PET are used to detect and localize PCa. B-mode or grayscale US is still the most extensively used PCa detection modality, although new scientific data are highlighting additional promising modalities. Previously utilized mainly for staging and recurrence detection, clinics worldwide are now using mpMRI for PCa detection via direct in-bore MRI-guided biopsy or MRI-US fusion-guided biopsy. CEUS and RTE have become promising US-guided PCa detection methods. This suggests a promising future for an integrated multimodality (mpUS and mpMRI) PCa detection strategy. PET imaging for PCa is useful for cancer staging, biochemical failure after radiation, and restricted diagnosis. Tumor biology and evolution are complex. To choose the best imaging method, one must understand tumor growth mechanisms. Figure 2 summarizes the tumor traits that imaging methods exploit. Grayscale or B-mode US modalities image zonal anatomical deficits produced by prostatic cancers. Doppler US and CEUS image tumor macro vascularity and micro vascularity because tumors are angiogenic. Prostate RTE relies on rigid PCa tissue. mpUS or mpUS-based imaging of PCa uses anatomical and functional US imaging techniques. Researchers worldwide are studying this. Standardizing intraprocedure mpUS imaging and lesion assessment may enable accurate, cost-effective office-based prostate biopsies.

PCa imaging has been most affected by mpMRI in recent years. Several studies have shown that direct MRI-guided biopsies or MRI-US fusion-guided biopsies increase clinically important cancer detection and decrease clinically insignificant cancer detection. This prevents under detection of malignant disease and over detection (and overtreatment) of indolent disease, which affects PCa care. mpMRI detects PCa using anatomical and functional methods. T2-weighted images show suspicious anatomical variations in normal prostate tissue, which may be caused by cancer; DWI measures the restricted Brownian motion of water molecules caused by increased cellularity of tumors; and dynamic contrast-enhanced imaging exploits angiogenesis-induced tumor vascularity. MR spectroscopic imaging can also detect prostate cancer-induced metabolite alterations. PET imaging helps detect biochemical relapse, PCa recurrence, and metastases. This uses several radiolabeled tracers. PET is also used with CT or MR to locate radiotracer uptake hot spots. Tumor biology determines radiotracer selection. The ¹⁸F-FDG tracer targets tumor glucose metabolism, the ¹⁸F ACBC-, choline-, and acetate-based tracers target molecules elevated and proliferating during tumor growth, and the PSMA-based tracers target ligand-receptor interactions in tumors with enhanced PSMA expression. In conclusion, cutting-edge imaging techniques have transformed PCa management, and more interesting research and advancements await.

4. CONCLUSION

Imaging is becoming an increasingly significant tool for both the early detection of prostate cancer and the management of the disease. This article provides a summary of the most important imaging modalities that are employed in the diagnosis and localization of prostate cancer, including multiparametric ultrasound, multiparametric magnetic resonance imaging, MRI-US fusion imaging, and PET imaging. The biological aspects of tumors, which are responsible for the justification of the application of particular imaging modalities, are given a lot of attention.

REFERENCES

- [1] Jemal, R. Siegel, E. Ward, T. Murray, J. Xu, and M. J. Thun, "Cancer statistics, 2007," *CA: A Cancer Journal for Clinicians*, vol. 57, no. 1, pp. 43–66, 2007.
- [2] E. D. Crawford and A. B. Barqawi, "Targeted focal therapy: a minimally invasive ablation technique for early prostate cancer," *Oncology*, vol. 21, no. 1, pp. 27–32, 2007.
- [3] M. R. Cooperberg, J. W. Moul, and P. R. Carroll, "The changing face of prostate cancer," *Journal of Clinical Oncology*, vol. 23, no. 32, pp. 8146–8151, 2005.

- [4] V. Scattoni, A. Zlotta, R. Montironi, C. Schulman, P. Rigatti, and F. Montorsi, "Extended and saturation prostatic biopsy in the diagnosis and characterization of prostate cancer: a critical analysis of the literature," *European Urology*, vol. 52, pp. 1309–1322, 2007.
- [5] Ohori M, Wheeler TM, Dunn JK, Stamey TA, Scardino PT. The pathological features and prognosis of prostate cancer detectable with current diagnostic tests. *J Urol*. 1994;152(5 pt 2):1714–1720.
- [6] Hodge KK, McNeal JE, Stamey TA. Ultrasound guided transrectal core biopsies of the palpably abnormal prostate. *J Urol*. 1989;142(1):66–70.
- [7] Hodge KK, McNeal JE, Terris MK, Stamey TA. Random systematic versus directed ultrasound guided transrectal core biopsies of the prostate. *J Urol*. 1989;142(1):71–74. 8
- [8] Bjurlin MA, Wysock JS, Taneja SS. Optimization of prostate biopsy: review of technique and complications. *Urol Clin North Am*. 2014;41(2):299–313.
- [9] Singh H, Canto EI, Shariat SF, et al. Predictors of prostate cancer after initial negative systematic 12 core biopsy. *J Urol*. 2004;171(5):1850–1854.
- [10] Taira AV, Merrick GS, Galbreath RW, et al. Performance of transperineal template-guided mapping biopsy in detecting prostate cancer in the initial and repeat biopsy setting. *Prostate Cancer Prostatic Dis*. 2010;13(1):71–77.
- [11] Zaytoun OM, Moussa AS, Gao T, Fareed K, Jones JS. Office based transrectal saturation biopsy improves prostate cancer detection compared to extended biopsy in the repeat biopsy population. *J Urol*. 2011;186(3):850–854.
- [12] Isariyawongse BK, Sun L, Banez LL, et al. Significant discrepancies between diagnostic and pathologic Gleason sums in prostate cancer: the predictive role of age and prostate-specific antigen. *Urology*. 2008;72(4):882–886.
- [13] Braeckman J, Autier P, Soviany C, et al. The accuracy of transrectal ultrasonography supplemented with computer-aided ultrasonography for detecting small prostate cancers. *BJU Int*. 2008;102(11):1560–1565.
- [14] Simmons LA, Autier P, Zat'ura F, et al. Detection, localization and characterisation of prostate cancer by prostate HistoScanning(TM). *BJU Int*. 2012;110(1): 28–35.
- [15] Schiffmann J, Manka L, Boehm K, et al. Controversial evidence for the use of HistoScanning in the detection of prostate cancer. *World J Urol*. 2015;33(12): 1993–1999.
- [16] Loch T. Computerized transrectal ultrasound (C-TRUS) of the prostate: detection of cancer in patients with multiple negative systematic random biopsies. *World J Urol*. 2007;25(4):375–380.
- [17] Halpern EJ, Frauscher F, Strup SE, Nazarian LN, O'Kane P, Gomella LG. Prostate: high-frequency Doppler US imaging for cancer detection. *Radiology*. 2002;225(1):71–77.
- [18] Sauvain JL, Sauvain E, Rohmer P, et al. Value of transrectal power Doppler sonography in the detection of low-risk prostate cancers. *Diagn Interv Imaging*. 2013;94(1):60–67.
- [19] Postema AW, Frinking PJ, Smeenge M, et al. Dynamic contrast-enhanced ultrasound parametric imaging for the detection of prostate cancer. *BJU Int*. 2015 Mar 6. doi: 10.1111/bju.13116.
- [20] Good DW, Stewart GD, Hammer S, et al. Elasticity as a biomarker for prostate cancer: a systematic review. *BJU Int*. 2014;113(4):523–534.
- [21] Zhang B, Ma X, Zhan W, et al. Real-time elastography in the diagnosis of patients suspected of having prostate cancer: a meta-analysis. *Ultrasound Med Biol*. 2014;40(7):1400–1407.
- [22] Zhai L, Madden J, Foo WC, et al. Acoustic radiation force impulse imaging of human prostates ex vivo. *Ultrasound Med Biol*. 2010;36(4):576–588.

- [23] Boehm K, Salomon G, Beyer B, et al. Shear wave elastography for localization of prostate cancer lesions and assessment of elasticity thresholds: implications for targeted biopsies and active surveillance protocols. *J Urol.* 2015;193(3):794–800.
- [24] Bhavsar A, Verma S. Anatomic imaging of the prostate. *Biomed Res Int.* 2014; 2014:9.
- [25] Turkbey B, Pinto PA, Mani H, et al. Prostate cancer: value of multiparametric MR imaging at 3 T for detection—histopathologic correlation. *Radiology.* 2010;255(1):89–99.
- [26] Tokuda J, Tuncali K, Iordachita I, et al. In-bore setup and software for 3T MRI-guided transperineal prostate biopsy. *Phys Med Biol.* 2012;57(18):5823–5840.
- [27] Tilak G, Tuncali K, Song SE, et al. 3T MR-guided in-bore transperineal prostate biopsy: a comparison of robotic and manual needle-guidance templates. *J Magn Reson Imaging.* 2015;42(1):63–71.
- [28] Sonn GA, Natarajan S, Margolis DJ, et al. Targeted biopsy in the detection of prostate cancer using an office based magnetic resonance ultrasound fusion device. *J Urol.* 2013;189(1):86–91.
- [29] Vourganti S, Rastinehad A, Yerram NK, et al. Multiparametric magnetic resonance imaging and ultrasound fusion biopsy detect prostate cancer in patients with prior negative transrectal ultrasound biopsies. *J Urol.* 2012;188(6):2152–2157
- [30] Marko J, Gould CF, Bonavia GH, Wolfman DJ. State-of-the-art imaging of prostate cancer. *Urol Oncol.* 2015 Jun 15. pii: S1078-1439(15)00239-2. doi: 10.1016/j.urolonc.2015.05.015.
- [31] Schuster DM, Taleghani PA, Nieh PT, et al. Characterization of primary prostate carcinoma by anti-1-amino-2-[[¹⁸F]-fluorocyclobutane-1-carboxylic acid (anti-3-[[¹⁸F] FACBC) uptake. *Am J Nucl Med Mol Imaging.* 2013;3(1): 85–96.
- [32] Bouchelouche K, Turkbey B, Choyke PL. Advances in imaging modalities in prostate cancer. *Curr Opin Oncol.* 2015;27(3):224–231.
- [33] Afshar-Oromieh A, Zechmann CM, Malcher A, et al. Comparison of PET imaging with a (⁶⁸Ga)-labelled PSMA ligand and (¹⁸F)-choline-based PET/ CT for the diagnosis of recurrent prostate cancer. *Eur J Nucl Med Mol Imaging.* 2014;41(1):11–20